RESEARCH ARTICLE

Nitrifiers and denitrifiers respond rapidly to changed moisture and increasing temperature in a pristine forest soil

Ute Szukics[1,2], Guy C.J. Abell[1,3], Verania Hödl[1], Birgit Mitter[1], Angela Sessitsch[1], Evelyn Hackl[1] and Sophie Zechmeister-Boltenstern[2]

[1]AIT Austrian Institute of Technology GmbH, Bioresources Unit, Seibersdorf, Austria; [2]Federal Research and Training Centre for Forests, Natural Hazards and Landscape, Vienna, Austria; and [3]CSIRO Marine and Atmospheric Research and Wealth from Oceans, National Research Flagship, Hobart, Tasmania, Australia

Correspondence: Ute Szukics, Federal Research and Training Centre for Forests, Natural Hazards and Landscape, Seckendorff-Gudent-Weg 8, A-1131 Wien, Austria. Tel.: +43 1 878381304; fax: +43 1 878381250; e-mail: ute_szukics@gmx.at

Received 20 March 2009; revised 1 February 2010; accepted 4 February 2010.
Final version published online 18 March 2010.

DOI:10.1111/j.1574-6941.2010.00853.x

Editor: Jim Prosser

Keywords
nitrification; denitrification; NO; N_2O emission; *nirK*; *amoA*; T-RFLP; qPCR.

Abstract

Complete cycling of mineral nitrogen (N) in soil requires the interplay of microorganisms performing nitrification and denitrification, whose activity is increasingly affected by extreme rainfall or heat brought about by climate change. In a pristine forest soil, a gradual increase in soil temperature from 5 to 25 °C in a range of water contents stimulated N turnover rates, and N gas emissions were determined by the soil water-filled pore space (WFPS). NO and N_2O emissions dominated at 30% WFPS and 55% WFPS, respectively, and the step-wise temperature increase resulted in a threefold increase in the NO_3^- concentrations and a decrease in the NH_4^+ concentration. At 70% WFPS, NH_4^+ accumulated while NO_3^- pools declined, indicating gaseous N loss. *AmoA*- and *nirK*-gene-based analysis revealed increasing abundance of bacterial ammonia oxidizers (AOB) with increasing soil temperature and a decrease in the abundance of archaeal ammonia oxidizers (AOA) in wet soil at 25 °C, suggesting the sensitivity of the latter to anaerobic conditions. Denitrifier (*nirK*) community structure was most affected by the water content and *nirK* gene abundance rapidly increased in response to wet conditions until the substrate (NO_3^-) became limiting. Shifts in the community structure were most pronounced for *nirK* and most rapid for AOA, indicating dynamic populations, whereas distinct adaptation of the AOB communities required 5 weeks, suggesting higher stability.

Introduction

Nitrification and denitrification represent key processes determining the availability and form of nitrogen (N) in soils and are held responsible for gaseous N losses as NO or N_2O, both of which act as potent greenhouse gases. The ability to denitrify is widespread among various microbial taxa, including phylogenetically diverse groups (Zumft, 1997). For instance, *nirK* and *nirS* genes, encoding the key enzyme nitrite reductase, have been assigned to unrelated affiliations (Philippot, 2002). Conversely, nitrification was long believed to be restricted to a monophyletic group of bacteria, until recent studies attributed environmental *amoA* homologues to members of the *Crenarchaeota* phylum within the domain Archaea (Treusch *et al.*, 2005). The interplay between nitrite reducers, ammonia-oxidizing bacteria (AOB) and ammonia-oxidizing archaea (AOA) is determined by environmental parameters such as soil temperature and soil water content (Wallenstein *et al.*, 2006; Avrahami & Bohannan, 2007). Nitrification and denitrification, which together complete the cycling of mineral N in soil, have optima under different environmental conditions, but may occur simultaneously (Gödde & Conrad, 1999).

Potential changes in the world's climate are expected to result in an increase in extreme events (Easterling *et al.*, 2000), including a higher frequency of intense precipitation, increases in extreme high temperatures, decreases in extreme low temperatures, heat waves and drought (Schär *et al.*, 2004; IPCC, 2007). The capacity of nitrifiers

FEMS MICROBIOLOGY ECOLOGY

and denitrifiers to respond to such short-term changes in the environment, corresponding NO and N_2O emissions and subsequent implications for mineral N balances are, however, poorly understood. Previous studies have reported rapidly altered activities of soil nitrifiers and denitrifiers in response to changing environmental conditions. Incubation for 5 days at temperatures up to 37 °C caused a marked decrease in NH_4^+ and an increase in NO_3^- concentrations in agricultural soils (Avrahami *et al.*, 2003). Despite the rapid stimulation of nitrification activity, a slow adaptation to changing soil temperature has been attributed to soil AOB. Community changes were detected after 16 weeks in agricultural soils and after 8–16 weeks in meadow soils (Avrahami & Conrad, 2003, Avrahami *et al.*, 2003), indicating decoupling of activity and community responses. Archaeal *amoA* communities have previously demonstrated higher dynamics by responding to soil temperature within 12 days of incubation at temperatures between 10 and 30 °C (Tourna *et al.*, 2008). The initiation of NO and N_2O production within minutes of wetting dry grassland soils (Davidson, 1992) demonstrated a rapid activation of denitrification in soil. However, a lack of response of denitrifying communities (*nosZ*) to changes in temperature and water content suggested a high stability of denitrifying communities (Stres *et al.*, 2008).

Whereas most previous studies of the effects of soil moisture and temperature have focused on investigating either activity responses, fluxes of N oxides or adaptations at the community/abundance level, the challenge of this study was to combine functional and structural responses with the aim of drawing a more complete picture of the interplay between nitrification and denitrification.

In order to explore short-term changes in N cycling processes in soil, we investigated the capacity of nitrifying (AOB and AOA) and denitrifying (nitrite reducing) functional groups to adapt to a changing environment. Changes in the gene abundance, community structure and related microbial activities were monitored continuously throughout a constant increase in temperature in soils at three water contents. The subject of the study was the pristine Rothwald spruce–fir–beech forest, which has experienced a long history of undisturbed evolution since the last ice age and represents the largest remnant of pristine temperate forests in Central Europe. The Rothwald forest has previously been shown to host a threefold higher diversity of microbiota than other natural forest soils in Austria (Hackl *et al.*, 2004). For this reason, the Rothwald forest offered a unique opportunity to study the responsiveness of putative nitrifiers and denitrifiers and the regulation of N balances under gradually changing environmental conditions in a well-equilibrated forest ecosystem.

Materials and methods

Soil sampling

In October 2004, samples of mineral soil were taken from the Rothwald forest, which comprises 460 ha of pristine forest located in a remote valley in Lower Austria at 1035 m above sea level. The Rothwald spruce–fir–beech forest is situated on dolomite bedrock and the soil type is Chromic Cambisol, with a pH value of 5.3 and a C : N ratio of 17.1. Mean annual precipitation amounts to 1759 mm and the average temperature is 5.5 °C (Hackl *et al.*, 2004). Ten individual samples (0–10 cm depth) were collected at intervals of 5 m along a 50-m transect. The 10 individual soil samples were sieved (2-mm mesh) and combined to form one homogenous soil sample in order to exclude variability in aeration and compaction.

Soil incubation

Soil microcosms were established in 15 stainless-steel soil cylinders of 7.5 cm diameter and 5 cm height, filled with approximately 120 g homogenized fresh soil. Soil water content was adjusted to either 30%, 55% or 70% water-filled pore space (WFPS), by drying in ambient air or wetting with distilled water using a syringe. Five replicates soil cores were established for each moisture level and were preincubated at 5 °C for 1 week with periodical readjustment of the water content. Soil temperature was increased weekly in four 5 °C increments from 5 to 25 °C. Three days after increasing the temperature, soil samples were taken from incubated soil cores for analysis of mineral N concentrations and N turnover rates. At each temperature, one soil core of each moisture level was sampled destructively for replicated determination of NH_4^+ and NO_3^- concentrations and measurement of N turnover processes (nitrate reductase activity, nitrification rate, N-mineralization) in four subsamples. N trace gas fluxes (NO, N_2O) were measured in four replicate soil cores at each moisture level. During the gas measurements, soil cores were maintained at the respective incubation temperature for 4 days. Following process measurements, soils were stored at -20 °C for subsequent DNA extraction.

Gas-flux analysis

The NO emission from the soil cores was measured after 4 days of incubation using a fully automated system operated by a personal computer as described by Schindlbacher *et al.* (2004). An incubator containing 13 temperature-controlled test chambers was linked to a chemo-luminescence nitrogen oxide analyzer (HORIBA-APNA-360). The soil cores were placed in individual test chambers, with one empty jar serving as a control. The NO concentration in the

flow-through stream of each vessel was analysed separately at intervals of 8 min, generating > 60 NO measurements per sample throughout the analyses.

For N_2O measurements, the soil cores were incubated in gas-tight test chambers (headspace volume 450 mL, $n = 4$) at controlled temperatures. Head-space gas samples of 15 mL were taken with a syringe immediately after closure, after incubation for 3 and 6 h. The gas samples were transferred to 10-mL evacuated glass vials, sealed with silicone grease and stored under water at 4 °C until analysis. Nitrous oxide concentration was analysed by GC (Hewlett-Packard 5890 Series II, injector: 120 °C, detector: 330 °C, oven: 120 °C, carrier gas: N_2) using a ^{63}Ni electron capture detector. Nitrous oxide flux was calculated from the linear increase in concentration over the incubation time and corrected for air temperature and pressure.

N turnover rates and mineral N pools

Nitrification and nitrate reductase activities were measured after 4 days of incubation and involved the addition of dissolved substrates or inhibitors to the individual assays. Compounds were applied in a 400 μL aqueous solution to 2.5 g soil aliquots of each treatment to maintain WFPS. This volume corresponded to the amount of water evaporating during 24 h of incubation (data not shown). Nitrate reductase activity was measured according to Schinner *et al.* (1996) using KNO_3 as a substrate (final concentration 0.0625 M) and dinitrophenol as an inhibitor of nitrite reductase. Preliminary tests showed optimal inhibition at a concentration of 7×10^{-3} mg dinitrophenol g^{-1}dry Rothwald soil (data not shown). The substrate–dinitrophenol solution was applied to 2.5 g soil aliquots of each treatment ($n = 6$) with a microsyringe, followed by mixing. Four replicates were kept at the respective temperature for 24 h and two samples, serving as blanks, were immediately frozen at −20 °C. Total NO_2^- from samples and blanks was extracted with 3 M KCl and analysed photometrically (μQuant, BIO TEC Instruments Inc.). Nitrate reductase activities were calculated according to Schinner *et al.* (1996). To measure the nitrification rate, $NaClO_3$ (0.234 M), serving as an inhibitor of NO_2^- oxidation (Belser & Mays, 1980), was applied to 2.5 g soil aliquots ($n = 6$). Two samples per treatment, serving as blanks, were frozen at −20 °C and four replicates were incubated for 24 h at the respective temperature. Nitrite was extracted with 2 M KCl and analysed photometrically. The nitrification rate was calculated as described by Schinner *et al.* (1996). The nitrite concentration of individual treatments was calculated from blanks (nitrification rate, nitrite reductase activity) using measured background NO_2^- concentration ($n = 4$). To measure the mineralization rate, acetylene was used as an inhibitor of ammonia oxidation (Berg *et al.*, 1982). Soil aliquots of 5 g ($n = 3$) were incubated in gas-tight glass flasks (volume 13 cm^3) under 3% acetylene-atmosphere. Ammonium was extracted before and after incubation at the respective temperature as described below and the mineralization rate was calculated according to Schinner *et al.* (1996). Ammonium, nitrite and nitrate were extracted from 5 g of fresh soil samples with 30 mL $CaCl_2$ (0.0125 M) and shaking for 30 min ($n = 3$). NH_4^+-N in filtered soil extracts was detected photometrically at 660 nm, while NO_3^--N was determined as NO_2^- after an overnight reduction with copper-sheathed granulated zinc at 210 nm (Schinner *et al.*, 1996).

DNA extraction and quantification of *nirK*, bacterial and archaeal *amoA* by real-time PCR

DNA was extracted from 0.5-g aliquots of incubated soil samples using the FastDNA Spin Kit for soil (Qbiogene). Three replicate DNA extractions of individual soil cores were pooled before PCR amplification. Functional marker genes encoding nitrite reductase (*nirK*), archaeal and bacterial ammonia monooxygenase (archaeal *amoA*, bacterial *amoA*) were quantified in triplicate by real-time PCR using an iCycler IQ (Biorad). The 25-μL PCR reaction mix contained 10 mg mL^{-1} bovine serum albumin (BSA), 0.675 μL dimethyl sulphoxide (DMSO), 12.5 μL of Q Mix (Biorad; 100 mM KCl, 40 mM Tris-HCl, 6 mM $MgCl_2$, 0.4 mM each of dNTP, 50 U mL^{-1} iTaq DNA polymerase, SybrGreen I, 20 nM fluorescein and stabilizer) and 25–50 ng template. Fluorescence acquisition was performed at 77 °C for *nirK*, at 81 °C for bacterial *amoA* and at 78 °C for archaeal *amoA*, where all primer dimers had melted, but specific products had not. To quantify *nirK*, 1 μL (of a 10 μM solution) of each PCR primer nirK1F (GGMATGGTKCC STGGCA) and nirK5R (GCCTCGATCAGRTTRTGG) was added to the PCR mix, resulting in a 514-bp product (Braker *et al.*, 1998). The cycling conditions were 95 °C for 3 min, six touch-down cycles of 15 s at 95 °C, 30 s at 63 °C (decreasing 1 °C per cycle) and 30 s at 72 °C, followed by 40 cycles of 15 s at 95 °C, then 58, 72 and 77 °C for 30 s each. Quantification of bacterial *amoA* fragments (491 bp) was performed using the primer pair amoA-1F (GGGGTTTCTACTGGTGGT) and amoA-2R (CCCCTCKGSAAAGCCTTCTTC) (Rotthauwe *et al.*, 1997), of which 1.25 μL (10 μM each) was added to the reaction mix. The cycling conditions were 95 °C for 3 min, followed by 45 cycles of 95, 57, 72 and 81 °C for 1 min each. The archaeal *amoA* gene real-time PCR reaction contained 0.75 μL (10 μM each) of the primers Arch-amoAF (STAATGGTCTGGCTTAGACG) and Arch-amoAR (GCGGCCATCCATCTGTATGT) (10 μM each) according to Francis *et al.* (2005), resulting in a 635-bp product. The cycling conditions were 95 °C for 5 min, followed by 45 cycles of 45 s at 95 °C, 45 s at 53 °C, 60 s at 72 °C and 60 s at 78 °C. Amplification of *nirS* using the primer pairs Cd3aF and R3cd according to Throbäck *et al.*

(2004) or nirS1F and nirS1R according to Braker *et al.* (1998) failed to generate a PCR product.

The abundances of *nirK*, bacterial and archaeal *amoA* genes were calculated as copy number g^{-1} dry soil. In addition, gene copy number ng^{-1} DNA was calculated and correlated to gene copy number g^{-1} soil. Plasmids containing the respective functional gene as an insert (*nirK*, bacterial *amoA* or archaeal *amoA*) were isolated from clones using Easy Prep Pro (Biozym). Standards for qPCR were generated by serial dilution of stocks of a known number of plasmids containing the respective functional gene. The reaction efficiencies of qPCRs were 94.5% (± 2.5) for *nirK*, 98% (± 2) for archaeal *amoA* and 76.5% (± 3.5) for bacterial *amoA* and the R^2-values were 0.99 for all runs. No inhibitory effect on qPCR amplification was detected when serially diluted Rothwald soil DNA was spiked with known concentrations of standard plasmids (*nirK*, AOA, AOB).

Community profiling by terminal restriction fragment length polymorphism (T-RFLP) analysis

For T-RFLP analysis, fluorescently end-labelled forward primers (carboxyfluorescein phosphoramidite marked FAM) were used for the amplification of *nirK* and bacterial and archaeal *amoA* genes. The primer sets used were nirK1F-FAM and nirK5R for amplifying *nirK*, amoA-1F-FAM and amoA-2R for bacterial *amoA* and Arch-amoAF-FAM and Arch-amoAR for archaeal *amoA*. PCR amplifications, performed in T1 thermocyclers (Biometra), involved an initial denaturation step at 95 °C for 5 min, followed by 38 cycles of 30 s at 95 °C, 40 s at 54.4 °C and 60 s at 72 °C, followed by a final elongation step of 72 °C for 5 min. Amplification was performed in 25-μL reactions containing 2.5 μL (2 μM each) of the primer set, 2.5 μL dNTPs (2 mM), 3 μL $MgCl_2$ (25 mM), 2.5 μg BSA (Sigma, 10 mg mL^{-1}), 1 μL DMSO, ~50 ng DNA, 1 U Firepol polymerase (Solis Biodyne) and 1 × reaction buffer provided with the enzyme.

To generate T-RFLP profiles, three replicate PCR reactions from each sample were pooled and purified using the Invisorb Spin PCRapid Kit (Invitek) before digestion, as recommended by Hartmann *et al.* (2007). FAM-marked bacterial and archaeal *amoA* PCR products were digested with RsaI restriction enzyme (Invitrogen) at 37 °C for 3–4 h. The FAM-marked *nirK* products were digested with TaqI restriction enzyme (Promega) at 65 °C for 3–4 h. Each digest was conducted in a 10-μL reaction volume containing 200 ng FAM-marked PCR product, 1 μL reaction buffer and 2 U of the respective restriction enzyme. Digests were purified using Sephadex columns. HIDI loading buffer (formamide) and GeneScan-500 ROX length standard for sizing DNA fragments in the 35–500-bp range (Applied Biosystems) were added to the digests, which were then denatured at 92 °C for 2 min before analysis on an ABI Prism 3100 Genetic Analyzer (Applied Biosystems). Terminal restriction fragments (T-RFs) for each sample were calculated as described previously (Abell *et al.*, 2010). Briefly, fragments of each gene were compared with the internal standard using the GENESCAN software package (version 3.7, Applied Biosystems) and only fragments between 50 and 600 bp were included in the analysis. The area of each peak was expressed as a percentage of the total peak area in the profile and peaks comprising $< 1.5\%$ of the total area were excluded from the analysis.

Statistical analysis

ANOVA was performed using the ANOVA multiple range test (STATGRAPHICS PLUS 5.0) on mineral N pools, N turnover processes, gene abundance and AOA : AOB ratios. An LSD test was used for comparison of samples with equal size numbers, while the Scheffé test was used for samples with varying numbers of replicates. Mineral N pools, N turnover rates and the abundance of the functional genes were subjected to principal component analysis (PCA) (SAS, enterprise guide 2). The significance of the relationships between parameters represented by vectors with similar or opposite orientation was explored via multiple-variable analysis (STATGRAPHICS PLUS 5.0).

Statistical analysis of T-RFLP data was performed on standardized, square-root transformed data using PRIMER 6 software (PRIMER-E, Plymouth, UK). Nonmetric multidimensional scaling (nmMDS) using the Bray–Curtis similarity calculation was used to demonstrate the relatedness of individual community profiles under different treatments (Kenkel & Orloci, 1986; Minchin, 1987). The similarity between treatments on the basis of T-RFLP profiles was calculated using the one-way univariate ANOSIM including 10 000 permutations, with significant differences considered at $P < 0.01\%$ (Clarke, 1993). A similarity percentage analysis (SIMPER) was used to identify the major T-RFs responsible for the differences observed between treatments. ANOVA (Scheffé test, 95% confidence) was used (Buckley & Schmidt, 2001) to identify differences in the T-RF abundance, presence or absence between specific treatments.

Results

Mineral N pools

The NO_3^- concentration at 30% and 55% WFPS increased (Fig. 1) with increasing soil temperature and was three times higher at 25 °C than at 5 °C. Under O_2-limiting conditions at 70% WFPS, the soil NO_3^- concentration decreased with increasing temperature and was 19 times lower at 25 °C than at 5 °C. As a consequence, the NO_3 concentration at 25 °C was 90 times higher at 30% and 55% WFPS than in soil at 70% WFPS. The increase in the NO_3^- concentration that

occurred coincided with an overall decrease in the NH_4^+ concentration with increasing soil temperature at 30% and 55% WFPS. This resulted in three- and sixfold lower NH_4^+ concentrations at 25 °C than at 5 °C and 30% and 55% WFPS (Fig. 1). At 15, 20 and 25 °C, the NH_4^+ concentrations were comparably high in soil at 70% WFPS. Consequently, at 25 °C, the NH_4^+ concentrations were five- and ninefold higher at 70% WFPS than at 30% WFPS and 55% WFPS. The nitrite concentration (data not shown) was lower than the NO_3^- and NH_4^+ concentrations. The maximum NO_2^- concentration was 2.4 μg NO_2^--N g^{-1} soil at 20 °C and 70% WFPS and 1.4 μg NO_2^--N g^{-1} soil at 15 °C and 55% WFPS. In all other treatments, the NO_2^- concentration was $\leq$ 1 μg NO_2^--N g^{-1} soil.

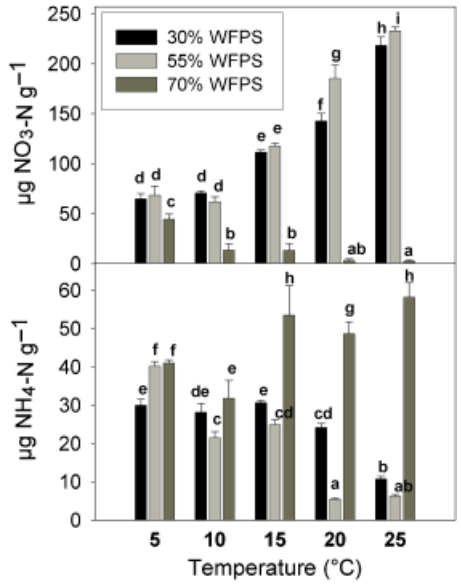

Fig. 1. Mean NO_3^- content (μg NO_3^--N g^{-1} soil) and mean NH_4^+ content (μg NH_4^+-N g^{-1} soil) at 30% WFPS, 55% WFPS and 70% WFPS and 5, 10, 15, 20 and 25 °C. Error bars represent SD. Different lower case characters represent significant differences, $P < 0.05$, LSD test.

N turnover processes

The mineralization rates at all water contents were greater at a higher soil temperature, resulting in up to 14-fold higher mineralization at 25 °C than at 5 °C (Table 1). The mineralization rate at 55% WFPS was the highest and increased uniformly with the soil temperature ($R^2 = 0.95$, $P < 0.0001$) between 5 and 25 °C. The increase in the mineralization rate at 30% WFPS and 70% WFPS was not uniform at each temperature level. The nitrification rate increased most rapidly at 55% WFPS (Table 1), resulting in 38 times higher nitrification rates at 25 °C than at 5 °C ($R^2 = 0.72$, $P < 0.0001$). In other treatments, the temperature response was masked by sample variability. Nitrification was the highest in soil at 55% WFPS when compared with 30% and 70% WFPS soils.

Nitrate reductase activity increased at higher soil temperatures at all water contents, with the highest activity at 55% WFPS (Table 1). At this moisture level, the highest (113-fold) increase in activity from 5 to 25 °C was also measured. At 30% WFPS activity increased steadily, but slowly ($R^2 = 0.84$, $P < 0.0001$). At 55% and 70% WFPS, where the conditions were more reductive, there was a sudden increase in activity at 20 and 25 °C compared with the lower temperatures.

N oxide gas fluxes

Nitric oxide emissions were the highest at 30% WFPS and the lowest at 70% WFPS, but increased at all water contents with increasing soil temperature (Fig. 2). The steepest (39-fold) increase in NO emission from 5 and 25 °C was measured at 55% WFPS. At all water contents, N_2O emissions tended to increase with increasing soil temperature (Fig. 2). N_2O emissions were the highest at 55% WFPS and a statistically significant (28-fold) exponential increase ($R^2 = 0.82$, $P < 0.0001$) occurred with increasing soil temperature. At 5 °C, N_2O peaked at 70% WFPS, with 79 and 23 times higher N_2O emissions than at 30% and 55% WFPS.

Table 1. Mean values of the mineralization rate (μg NH_4^+-N g^{-1} day^{-1}), nitrate reductase activity (μg N g^{-1} day^{-1} h^{-1}) and nitrification rate (ng N g^{-1} day^{-1}) in the Rothwald soil at 30% WFPS, 55% WFPS and 70% WFPS and 5, 10, 15, 20 and 25 °C

	Mineralization						Nitrate reductase						Nitrification					
T (°C)	30% WFPS		55% WFPS		70% WFPS		30% WFPS		55% WFPS		70% WFPS		30% WFPS		55% WFPS		70% WFPS	
5	0.7	abc	−0.3	a	0.4	ab	−0.1	a	0.1	a	−0.2	a	−1.8	a	79.5	ab	122.8	abc
10	0.1	ab	1.5	abc	4.0	de	0.8	abc	1.2	abc	0.0	a	183.3	abc	529.8	abc	−14.3	abc
15	1.5	abc	2.5	bcd	−0.8	ab	1.8	abc	3.1	bc	0.2	ab	48.4	abc	985.2	bc	106.8	abc
20	1.5	abc	4.3	def	3.0	cd	2.5	abc	13.3	e	10.1	d	452.4	abc	2404.2	d	1063.8	c
25	4.8	def	6.5	f	5.4	ef	3.3	c	14.2	e	7.8	d	398.5	abc	3014.8	d	629.0	abc

Different lower case characters represent significant differences, $P < 0.05$.

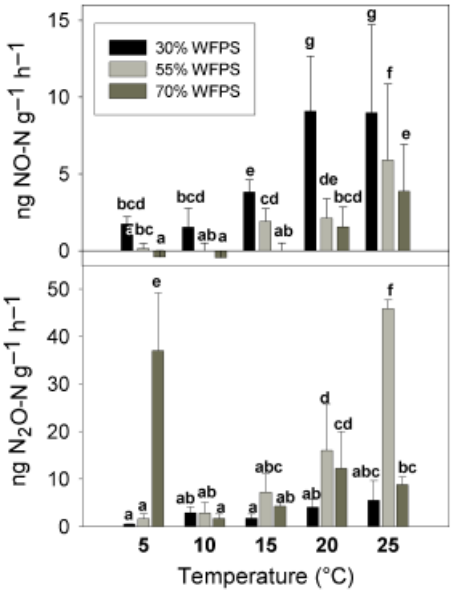

Fig. 2. Mean NO emission (ng NO-N g^{-1} h^{-1}) and mean N_2O emission (ng N_2O-N g^{-1} h^{-1}) at 30% WFPS, 55% WFPS and 70% WFPS and 5, 10, 15, 20 and 25 °C. Error bars represent SD. Different lower case characters represent significant differences, $P < 0.05$, Scheffé test.

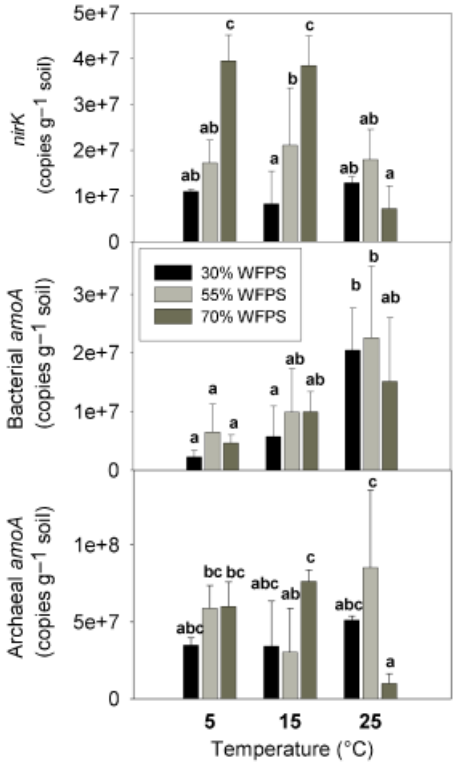

Fig. 3. Mean abundance of *nirK*, bacterial *amoA*, archaeal *amoA* genes (copies g^{-1} soil) at 30% WFPS, 55% WFPS and 70% WFPS and 5, 15 and 25 °C. Error bars represent SD. Different lower case characters represent significant differences at the 95% confidence level, $P < 0.05$, LSD test.

Quantification of *nirK*, archaeal and bacterial *amoA* genes

The abundance of *nirK* genes ranged from 6.4×10^6 to 4.0×10^7 copies g^{-1} soil within soils at the various WFPS levels (Fig. 3). At 70% WFPS, *nirK* gene copy numbers were the highest at 5 and 15 °C, but *nirK* abundance at 25 °C decreased fivefold compared with lower temperatures. At 5 and 15 °C, *nirK* genes were also more abundant at 70% WFPS than at 55% and 30% WFPS. A significant overall temperature effect on the *nirK* gene abundance was not observed.

Bacterial *amoA* gene copy numbers ranged from 2.4×10^6 to 2.2×10^7 copies g^{-1} and increased with increasing soil temperature (Fig. 3). From 5 to 25 °C, bacterial *amoA* abundance increased three- and ninefold at 55% and 30% WFPS, respectively. The soil water content had no significant effect on bacterial *amoA* gene abundance. Archaeal *amoA* genes were detected in high abundances, ranging from 1.1×10^7 to 8.1×10^7 copies g^{-1} soil (Fig. 3). At 70% WFPS, the archaeal *amoA* gene abundance was eight times higher at 15 °C than at 25 °C. A significant overall effect of soil water content and temperature on the abundance of archaeal *amoA* genes was, however, not observed. The interpretation of the qPCR results was the same whether expressed as gene copies ng^{-1} DNA or copies g^{-1} soil, and there was a strong linear relationship between the two measures (AOA: $R^2 = 0.90$, AOB: $R^2 = 0.61$, *nirK*: $R^2 = 0.89$; $P < 0.0001$). Archaeal *amoA* genes at different soil temperatures were between 0.7 and 15.5 times more abundant than bacterial *amoA* genes. Archaeal *amoA* abundance comprised 90–94%, 75–88% and 40–79% of the total *amoA* abundance at 5, 15 and 25 °C, respectively, indicating an effect of temperature on the AOA : AOB ratio, which decreased significantly with increasing soil temperature at 70% WFPS ($P = 0.001$). At 30% WFPS, the AOA : AOB ratios were lower at 15 and 25 °C than at 5 °C ($P < 0.05$). The same trend was observed for soil at 55% WFPS, although the effect was not significant ($P = 0.1$).

T-RFLP community analysis

NirK-gene-based community analysis revealed a total of 61 peaks across all profiles, with one major peak (200 bp) and three peaks (74, 103 and 244 bp length) having respective abundances of 20% and > 5% of the total abundance. Samples subjected to the same treatment clearly clustered in an nmMDS plot with a stress value of 0.07 (Fig. 4a). Variation in the *nirK* community structure with different water contents was observed throughout incubation with increasing temperature (global $R = 0.55$, $P = 0.01$). ANOSIM

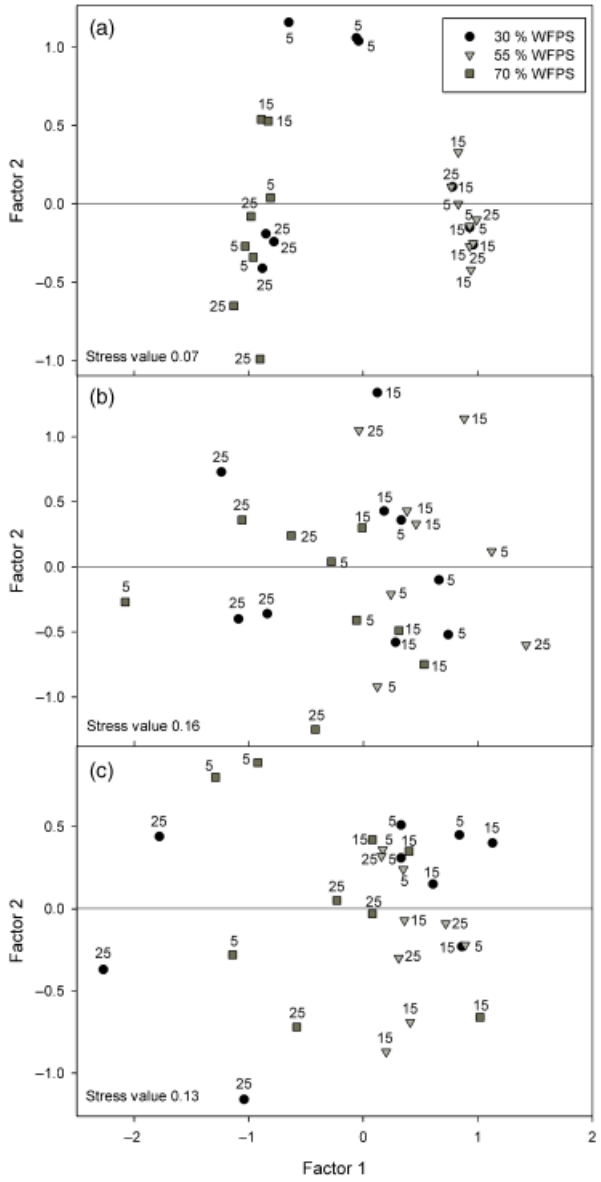

Fig. 4. Plots (nmMDS) based on Bray–Curtis similarities showing the relative similarities within (a) *nirK* and (b) bacterial *amoA* and (c) archaeal *amoA* T-RFLP profiles at 30% WFPS, 55% WFPS and 70% WFPS and 5, 15 and 25 °C. Numbers in the plot (5, 15, 25) represent the respective incubation temperatures.

analysis indicated an interactive effect of water content and temperature (global $R = 0.69$, $P = 0.01\%$). The *nirK* community structure varied according to the water content at all incubation times and temperatures (Table 2). The *nirK* communities at 30% WFPS, 55% WFPS and 70% WFPS differed from each other after 1 week of incubation at 5 °C ($R = 1$, $P = 0.01$). The major difference between treatments was attributed to a number of T-RFs (60, 101, 103, 135, 242, 244 and 387 bp length), as their occurrence varied significantly with the water content ($P < 0.001$). After 3 weeks of incubation with increasing temperature (up to 15 °C), the *nirK* community structure at 70% WFPS differed significantly from those at 55% WFPS and 30% WFPS ($R = 1$, $P = 0.01$) due to T-RFs 101, 242 and 387 bp in length, which were highly abundant at 70% WFPS, but not detected at 55% WFPS and 30% WFPS ($P < 0.0001$). After 5 weeks of incubation with increasing temperature (up to 25 °C), the *nirK* community structure at 55% WFPS differed from those at 30% WFPS and 70% WFPS ($R = 1$, $P = 0.01$), due to T-RFs of 60, 101 and 244 bp length, whose occurrence varied significantly between water levels at 25 °C ($P < 0.001$). The *nirK* community structure at 30% WFPS varied with the incubation time and increasing temperature and differed at 5, 15 and 25 °C ($R = 1$, $P = 0.01$) due to differences in the occurrence of T-RFs of 60, 101, 244, 242, 74, 103, 387 and 135 bp ($P < 0.001$).

Table 2. Differences in the T-RFLP patterns of Rothwald soil at 30% WFPS, 55% WFPS and 70% WFPS and 5, 15, 25 °C. Most significant different T-RFLP profiles according to (a) water contents and (b) incubation temperatures are highlighted (*R*-value > 0.6)

a	% WFPS	5 °C	15 °C	25 °C
nirK	30 vs. 55			$R = 1$
	30 vs. 70	$R = 1$	$R = 1$	
	55 vs. 70			$R = 1$
AOB	30 vs. 55			$R = 0.67$
	30 vs. 70	$R = 0.41$		
	55 vs. 70	$R = 0.24$		
AOA	30 vs. 55			$R = 0.96$
	30 vs. 70	$R = 0.96$		$R = 0.78$
	55 vs. 70	$R = 0.89$		
b	T (°C)	30% WFPS	55% WFPS	70% WFPS
nirK	5 vs. 15			
	5 vs. 25	$R = 1$		
	15 vs. 25			
AOB	5 vs. 15		$R = 0.59$	
	5 vs. 25	$R = 1$	$R = 0.58$	
	15 vs. 25	$R = 0.78$		$R = 0.67$
AOA	5 vs. 15	$R = 0.41$		$R = 0.78$
	5 vs. 25	$R = 1$		$R = 0.63$
	15 vs. 25	$R = 1$		$R = 0.26$

Respective *R*-values are given ($P < 0.01$).

Bacterial *amoA* community profiles showed 27 peaks across all profiles including four dominant peaks at 250, 273, 376 and 485 bp length and three peaks (268, 274 and 373 bp) that comprised > 10% and > 5% of the total abundance, respectively. One replicate from the treatment group 55% WFPS at 25 °C contained an outlier that was eliminated before analysis. The nmMDS plot with a stress value of 0.16 indicated differences between treatments (Fig. 4b), which were further supported by an ANOSIM test demonstrating an interactional effect of WFPS and increasing temperature (global $R = 0.36$, $P = 0.02\%$). SIMPER

analysis indicated a range of T-RFs responsible for the differences between treatments, of which only one (378 bp) showed a significant variation between the treatments ($P < 0.0001$). The T-RF of 378 bp was abundant at 25 °C and 30% WFPS ($P < 0.0001$), but absent in the other treatments. At 30% WFPS, AOB profiles varied according to the incubation time and temperature, so that AOB communities at 25 °C differed in structure from those at 5 °C ($R = 1$, $P = 0.01$) and 15 °C ($R = 0.78$ $P = 0.01$), incubated for 5, 1 and 3 weeks, respectively (Table 2). SIMPER analysis indicated that approximately 9% of the difference between treatments was attributed to a T-RF 378 bp in length. After 5 weeks of incubation (up to 25 °C), AOB communities at 55% WFPS differed from those at 30% WFPS ($R = 0.67$, $P = 0.01$). At 70% WFPS, the AOB community structures at 25 and 15 °C were different ($R = 0.67$, $P = 0.01$). SIMPER analysis revealed a range of T-RFs accounting for this difference, but none demonstrated significantly increased abundance in any of the treatments.

Archaeal *amoA* community profiles contained 47 T-RFs across all profiles, of which four dominant fragments (58, 60, 138 and 300 bp length) and a further three fragments (130, 170, 196 bp) comprised $>$ 10% and of $>$ 5% of the total abundance, respectively. A significant difference between some treatments was demonstrated by nmMDS analysis, with a stress value of 0.13 (Fig. 4c). ANOSIM analysis indicated a significant interactive effect of water content and increasing temperature on archaeal *amoA* community structure (global $R = 0.36$, $P = 0.01\%$). Subsequent SIMPER analysis and one-way ANOVA suggested that this difference was due to variability in the dominance of four T-RF fragments (67, 138, 283 and 490 bp). At 70% WFPS, AOA patterns varied with the incubation time and temperature, such that AOA communities at 5 °C differed from those at 15 °C ($R = 0.78$, $P = 0.01$) and 25 °C ($R = 0.63$, $P = 0.01$) after 1, 3 and 5 weeks of incubation, respectively (Table 2). At 70% WFPS, T-RFs 283 and 67 bp in length were present and highly abundant at 5 °C, but absent or of negligible abundance at 15 and 25 °C ($P < 0.001$). After 1 week of incubation at 5 °C, the AOA community at 70% WFPS was different from those at 30% WFPS ($R = 0.96$, $P = 0.01$) and 55% WFPS ($R = 0.89$, $P = 0.01$). Three T-RFs 67, 138 and 283 bp in length accounted for 6%, 10% and 7% of these differences, respectively. At 5 °C, T-RFs 67 and 283 bp in length were abundant at 70% WFPS, but absent at 55% WFPS and 30% WFPS ($P < 0.001$), while the 138 bp T-RF was abundant at 30% WFPS and 55% WFPS, but not at 70% WFPS ($P = 0.0003$). After 5 weeks of incubation (up to 25 °C), AOA communities at 30% WFPS differed from those at 55% WFPS ($R = 0.96$, $P = 0.01$) and 70% WFPS ($R = 0.78$, $P = 0.01$). Two T-RFs 67 and 490 bp in length were most abundant at 25 °C and 30% WFPS, but absent at 55% and 70% WFPS ($P < 0.0001$). In soil at 30% WFPS, the AOA communities differed according to the incubation time and temperature, so that AOA patterns at 25 °C differed from those at 5 °C ($R = 1$, $P = 0.01$) and 15 °C ($R = 1$, $P = 0.01$). These differences can be partially explained by the T-RF of 490 bp, which, at 30% WFPS, was most abundant at 25 °C, but absent at 5 °C and 15 °C ($P < 0.0001$), and by the T-RF 138 bp in length, which was abundant at 5 °C, but of negligible abundance at 25 °C ($P = 0.0003$).

PCA

PCA of the N concentration, process rate and gene abundance data explored three factors with eigenvalues $>$ 1, which together accounted for 79.5% of the variability in the data. In a PCA plot of two factors that together explained 68% of the variability, individual samples clustered according to the treatment (Fig. 5). Individual samples incubated at 5 and 15 °C had mostly negative *y*-values, while samples incubated at 25 °C had mostly positive *y*-values, resulting in a temperature gradient running along the *y*-axis. The position of individual samples respective to the vectors indicated the key parameters contributing to the differences between the treatments. The *nirK* abundance was the key determinant at 70% WFPS, with samples incubated at 5 and 15 °C clustering alongside the *nirK* vector. Soil at 30% WFPS, located on the left side of the *y*-axis, was ordinated with higher NO emissions.

Vectors with a similar orientation indicated a relationship between the parameters analysed, which was further explored by statistical analysis. NO_3^- and NH_4^+ were negatively

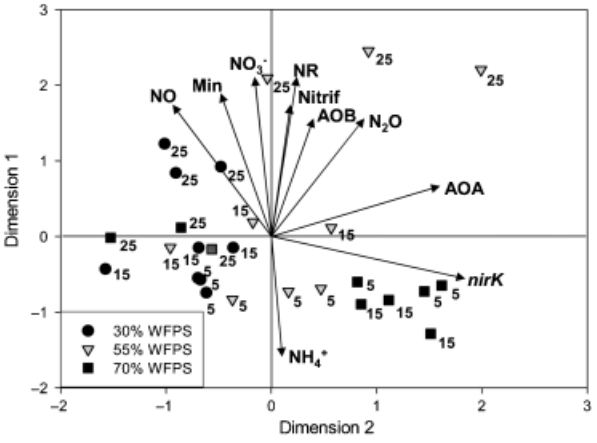

Fig. 5. PCA of mineral N pools, process data and real-time PCR data at 30% WFPS, 55% WFPS and 70% WFPS and 5, 15 and 25 °C. Arrows represent the abundance of *nirK* (*nirK*), bacterial *amoA* (AOB) and archaeal *amoA* (AOA) genes, the mineralization rate (Min), nitrate reductase activity (NR), nitrification rate (Nitrif), contents of nitrate (NO_3^-) and ammonium (NH_4^+) and emissions of nitric oxide (NO) and nitrous oxide (N_2O).

related ($R^2 = -0.96$, $P < 0.05$) as suggested by the opposing orientations of the respective vectors in the PCA plot. The nitrate concentration was closely related to the NO emission rate ($R^2 = 0.69$, $P < 0.001$), nitrification rate ($R^2 = 0.56$, $P < 0.001$) and mineralization rate ($R^2 = 0.55$, $P < 0.001$) and correlated positively with AOB abundance ($R^2 = 0.52$, $P < 0.05$), nitrate reductase activity ($R^2 = 0.49$, $P < 0.05$) and N_2O emission rate ($R^2 = 0.34$, $P < 0.05$). In contrast, the NH_4^+ concentration was negatively related to the NO emission rate ($R^2 = -0.58$, $P < 0.0001$) and correlated negatively with the nitrification rate ($R^2 = -0.49$, $P < 0.05$), AOB gene abundance ($R^2 = -0.38$, $P < 0.05$) and nitrate reductase activity ($R^2 = -0.37$, $P < 0.05$).

Discussion

Soil moisture and temperature effects on N turnover processes

A gradual increase in soil temperature from 5 to 25 °C induced a rapid stimulation of N cycling rates and a shift in the balance of NO_3^- and NH_4^+ concentrations at all three moisture levels. Different processes were driving N cycling at the various soil water contents, resulting in changes in the availability of mineral N forms. During the series of weekly temperature increases, NO_3^- steadily accumulated in dry and moist soils. The nitrification rate and NO_3^- concentration increased most rapidly at a moderate water content (55% WFPS), at which the NH_4^+ concentration and water supply appeared to be favourable. However, in wet soil, the NO_3^- pool decreased continuously and was almost depleted at 25 °C. This nitrate loss observed under wet conditions can be attributed to complete denitrification and release of N_2 gas into the atmosphere (Davidson & Swank, 1986). Soil moisture was the major determinant of N_2O and NO emissions from the Rothwald soil. The production of NO mostly in dry soils during nitrification, and of N_2O in moist soils due to denitrification, have been proposed by Firestone & Davidson (1989). Our study broadly confirms these theories because most NO was emitted at 30% WFPS, while N_2O emissions were the highest at 55% WFPS. This moisture effect was not reflected in the abundances of AOB and AOA. However, *nirK* abundance clearly increased with increasing water content until the NO_3^- supply became limiting. Despite the high *nirK* abundance at 70% WFPS, suggesting favourable nitrite-reducing conditions, the lowest amounts of NO and medium N_2O levels were emitted under these conditions. Following the onset of anaerobiosis, N_2O reduction exceeds the rate of N_2O production, with N_2 being the dominant product of denitrification (Firestone & Tiedje, 1979). We suggest that the intermediates NO and N_2O were not released under increasingly anoxic conditions at 70% WFPS, but were further reduced to N_2, because many nitrite reducers also possess other denitrification genes, enabling them to perform several steps of the denitrification pathway (Philippot, 2002). Precipitation events, in the same way as experimental wetting, may induce sudden N_2O peaks from the Rothwald forest soil, as also reported for dry grassland soils (Davidson, 1992) and for Amazon forest soils (Garcia-Montiel *et al.*, 2003). Temporally high NO_3^-, but low NH_4^+ availability was observed as a consequence of the low water availability and the high temperature in the Rothwald soil. Conversely, wet conditions seem likely to cause NH_4^+ to accumulate, whereas a strong decline in NO_3^- pools may occur even in cold seasons. This implies that N gas emissions in wet soils can be high even at low temperatures, as indicated by a high N_2O peak at 5 °C and 70% WFPS. Peak N_2O emissions from forest soils at 0 °C (Öquist *et al.*, 2004) have been attributed to the suppression of N_2O reductase at low temperatures, causing a shift in the N_2O to N_2 ratio towards enhanced N_2O emission (Dörsch & Bakken, 2004). Stres *et al.* (2008) reported persistent N_2O emissions at a low temperature and a high water content during 12 weeks of incubation, noting that N_2O emission in cold soils may be controlled by nitrification (Öquist *et al.*, 2007) as the NO_3^- contents were not depleted.

Structure and abundance of functional communities responding to soil moisture and temperature

Activity responses were accompanied by adaptations of microbial community structures and resulted in significant shifts in the functional gene abundances of AOB and AOA and nitrite reducers. Of all three groups, nitrite reducers showed the highest responsiveness to environmental changes. The abundance of potential nitrite reducers increased most rapidly and their community structure shifted most markedly in response to changes in the soil temperature and water content. Soil water content had a significant impact on nitrite reducers, as the *nirK* community structure varied according to the water content at all temperature increments and *nirK* gene copy numbers increased with increasing water content until NO_3^- became limiting. In contrast to the distinct response of Rothwald forest soil denitrifiers, only minor changes in the *nosZ* denitrifier community structure were observed in fen grassland during 12 weeks of incubation at modified soil water contents and soil temperatures (Stres *et al.*, 2008). The Rothwald forest was characterized as extraordinarily rich in nutrients, in comparison with 11 natural Austrian forests, hosting high microbial biomass and showing strong internal nutrient cycling (Hackl *et al.*, 2004a, b, 2005). The rapid community response of denitrifiers to variations in soil parameters may originate from particular characteristics of this pristine forest soil.

AOA in the Rothwald soil demonstrated a capacity to respond to environmental changes within a short time span. AOA communities differed in structure under extreme conditions, in wet soil (70% WFPS) at a low temperature (5 °C) or in dry soil (30% WFPS) at increasing temperature up to 25 °C. The rapid community adaptation under wet conditions, which was detectable after only 1 week at 5 °C, indicates the sensitivity of AOA to a high water content. Accordingly, the sensitivity of AOA to reductive conditions was suggested by the significant decrease in archaeal *amoA* abundance at 70% WFPS and 25 °C, where conditions were likely oxygen limited. In contrast to previously described AOA community shifts in response to temperature variation (Tourna *et al.*, 2008) and despite temperature being considered a key factor determining microbial growth, archaeal *amoA* gene abundance was not affected uniformly by temperature in Rothwald soil.

AOA were more dynamic than AOB communities, which appeared to be more stable, with less distinct differences in the community structure before 5 weeks of incubation with gradually increasing temperature. This may indicate an initial shift in the AOB community structure, whose adaptation has been reported to require several weeks. Avrahami *et al.* (2003) demonstrated, using denaturing gradient gel electrophoresis (DGGE) analysis, that incubation times of at least 16 weeks were required for AOB to adapt to changing environmental conditions in agricultural soils. DGGE analysis demonstrated that high fertilization treatments induced community shifts after only 6.5–12 weeks of incubation (Avrahami *et al.*, 2003), indicating ammonia as a selective factor for the community response of ammonia oxidizers. In a more recent study, community shifts of AOB were induced after a 7-week incubation of grassland soils and could be detected using T-RFLP analysis, but not using less-sensitive DGGE techniques (Avrahami & Bohannan, 2007), indicating different results with different fingerprinting techniques (Moeseneder *et al.*, 1999). However, AOB communities generally appeared to be more stable than AOA and may represent the K strategists among the nitrifiers in the Rothwald soil. A high potential for heterotrophic nitrification has been ascribed previously to acidic soils at pH 4–6 (Schimel *et al.*, 1984; Pedersen *et al.*, 1999). In the Rothwald soil, heterotrophic nitrification may be of only minor importance, because a strong negative correlation between NH_4^+ and NO_3^- concentrations indicated that NH_4^+ may represent the main source for NO_3^- production through autotrophic nitrification.

Consistent with the previous findings (Leininger *et al.*, 2006), AOA were more abundant than AOB in the Rothwald soil. However, the relative abundance of AOB in the Rothwald soil increased with increasing soil temperature in wet soils. At 5 °C, bacterial *amoA* genes comprised only ~10% of the total *amoA* gene abundance, but their relative abundance increased significantly at higher soil temperatures. This change in the AOA : AOB *amoA* gene abundance ratio resulted from a stimulation of AOB growth at elevated soil temperatures, while AOA abundance did not increase. He *et al.* (2007) found that both AOB and AOA *amoA* gene copy numbers were higher in summer than in winter in Chinese upland red soil, indicating a seasonal effect on both groups of ammonia oxidizers. However, divergent responses of AOA and AOB to soil pH (Nicol *et al.*, 2008), salinity (Santoro *et al.*, 2008), N fertilization (Shen *et al.*, 2008) and soil temperature and moisture in the present study provide evidence for the existence of AOA and AOB in distinct niches.

The observed shifts in the microbial community structure and changing abundances of *nirK*, bacterial and archaeal *amoA* genes suggest an impact on N cycling by altering the potential to reduce nitrate or oxidize ammonia, respectively. However, the conversion of inorganic N forms by nitrifiers and denitrifiers serves different purposes. Changes in the abundance and community structure of the mostly heterotrophic denitrifiers may relate to the uptake rates of organic C, rather than resulting from denitrification. Conversely, AOB as chemolithotrophic autotrophs have low growth rates (Ferguson *et al.*, 2007). AOA are still metabolically uncharacterized, but are believed to grow either autotrophically or mixotrophically (Hallam *et al.*, 2006; Prosser & Nicol, 2008). Consequently, the ability to transform inorganic N forms depends on the availability of the respective C source required.

Conclusion

The results of this study showed that short-term changes in the precipitation regime and soil temperature may rapidly affect the activity of both nitrifiers and denitrifiers, accompanied by changes in the source/sink strength of soils for N oxides and the availability of mineral N forms in forest ecosystems. General stimulation of N turnover rates was observed as temperatures were increased. Different processes were driving N cycling at the various water contents, resulting in variable mineral N balances. This study clearly demonstrated the different capacities of functional groups involved in N cycling to respond to short-term changes in the soil environment.

Acknowledgements

This study was supported by the Austrian Science Fund (FWF). We thank Brigitte Schraufstädter, Michael Pfeffer, Thomas Gschwantner, Barbara Kitzler, Katrin Ripka and Andreas Schindlbacher for their contributions. We are grateful to Jim Prosser for proof-reading and editorial suggestions.

References

Abell GCJ, Revill AT, Smith C, Bissett AP, Volkman JK & Robert SS (2010) Archaeal ammonia oxidizers and *nirS*-type denitrifiers dominate sediment nitrifying and denitrifying populations in a subtropical macrotidal estuary. *ISME J* **4**: 286–300.

Avrahami S & Bohannan BJM (2007) Response of *Nitrosospira* sp. strain AF-like ammonia oxidizers to changes in temperature, soil moisture content, and fertilizer concentration. *Appl Environ Microb* **73**: 1166–1173.

Avrahami S & Conrad R (2003) Patterns of community change among ammonia oxidizers in meadow soils upon long-term incubation at different temperatures. *Appl Environ Microb* **69**: 6152–6164.

Avrahami S, Liesack W & Conrad R (2003) Effects of temperature and fertilizer on activity and community structure of soil ammonia oxidizers. *Environ Microbiol* **5**: 691–705.

Belser LW & Mays EL (1980) Specific inhibition of nitrite oxidation by chlorate and its use in assessing nitrification in soils and sediments. *Appl Environ Microb* **39**: 505–510.

Berg P, Klemedtsson L & Rosswall T (1982) Inhibitory effect of low partial pressures of acetylene on nitrification. *Soil Biol Biochem* **14**: 301–303.

Braker G, Fesefeldt A & Witzel KP (1998) Development of PCR primer systems for amplification of nitrite reductase genes (*nirK* and *nirS*) to detect denitrifying bacteria in environmental samples. *Appl Environ Microb* **64**: 3769–3775.

Buckley DH & Schmidt TM (2001) The structure of microbial communities in soil and the lasting impact of cultivation. *Microb Ecol* **42**: 11–21.

Clarke KR (1993) Non-parametric multivariate analyses of changes in community structure. *Aust J Ecol* **18**: 117–143.

Davidson EA (1992) Sources of nitric oxide and nitrous oxide following wetting of dry soil. *Soil Sci Soc Am J* **56**: 95–102.

Davidson EA & Swank WT (1986) Environmental parameters regulating gaseous nitrogen losses from two forested ecosystems via nitrification and denitrification. *Appl Environ Microb* **52**: 1287–1292.

Dörsch P & Bakken LR (2004) Low-temperature response of denitrification: comparison of soils. *Eurasian Soil Sci* **37**: 102–106.

Easterling DR, Evans JL, Groisman PY, Karl TR, Kunkel KE & Ambenje P (2000) Observed variability and trends in extreme climate events: a brief review. *B Am Meteorol Soc* **81**: 417–425.

Ferguson SJ, Richardon DJ & Van Spanning RJM (2007) Biochemistry and molecular biology of nitrification. *Biology of the Nitrogen Cycle* (Bothe H, Ferguson SJ & Newton WE, eds), pp. 209–221. Elsevier, Amsterdam.

Firestone MK & Davidson EA (1989) Microbiological basis of NO and N_2O production and consumption in soil. *Exchange of Trace Gases Between Terrestrial Ecosystems and the Atmosphere* (Andreae MO & Schimel DS, eds), pp. 7–21. Wiley, Berlin.

Firestone M & Tiedje JM (1979) Temporal change in nitrous oxide and dinitrogen from denitrification following onset of anaerobiosis. *Appl Environ Microb* **38**: 673–679.

Francis CA, Roberts KJ, Beman JM, Santoro AE & Oakley BB (2005) Ubiquity and diversity of ammonia-oxidizing archaea in water columns and sediments of the ocean. *PNAS* **102**: 14683–14688.

Garcia-Montiel DC, Steudler PA, Piccolo M, Neill C, Melillo J & Cerri CC (2003) Nitrogen oxide emissions following wetting of dry soils in forest and pastures in Rondonia, Brazil. *Biogeochemistry* **64**: 319–336-.

Gödde M & Conrad R (1999) Immediate and adaptational temperature effects on nitric oxide production and nitrous oxide release from nitrification and denitrification in two soils. *Biol Fert Soils* **30**: 33–40.

Hackl E, Bachmann G & Zechmeister-Boltenstern S (2004a) Microbial nitrogen turnover in soils under different types of natural forest. *Forest Ecol Manag* **188**: 101–112.

Hackl E, Zechmeister-Boltenstern S, Bodrossy L & Sessitsch A (2004b) Comparison of diversities and compositions of bacterial populations inhabiting natural forest soils. *Appl Environ Microb* **70**: 5057–5065.

Hackl E, Pfeffer M, Donat C, Bachmann G & Zechmeister-Boltenstern S (2005) Composition of the microbial communities in the mineral soil under different types of natural forests. *Soil Biol Biochem* **37**: 661–671.

Hallam SJ, Mincer TJ, Schleper C, Preston CM, Roberts KJ, Richardson PM & DeLong EF (2006) Pathways of carbon assimilation and ammonia oxidation suggested by environmental genomic analyses of marine Crenarchaeota. *PLoS Biol* **4**: 520–536.

Hartmann M, Enkerli J & Widmer F (2007) Residual polymerase activity-induced bias in terminal restriction fragment length polymorphism analysis. *Environ Microbiol* **9**: 555–559.

He J, Shen J, Zhang L, Zhu Y, Zheng Y, Xu M & Di H (2007) Quantitative analyses of the abundance and composition of ammonia-oxidizing bacteria and ammonia-oxidizing archaea of a Chinese upland red soil under long-term fertilization practices. *Environ Microbiol* **9**: 2364–2374.

IPCC (2007) Climate Change 2007: Synthesis Report. Contribution of Working Groups I, II and III to the Fourth Assessment Report of the Intergovernmental Panel on Climate Change [Core Writing Team, R.K. Pachauri & A. Reisinger, (eds.)]. 104 pp. IPCC, Geneva, Switzerland.

Kenkel NC & Orloci L (1986) Applying metric and nonmetric multidimensional scaling to some ecological studies: some new results. *Ecology* **67**: 919–928.

Leininger S, Urich T, Schloter M *et al.* (2006) Archaea predominate among ammonia-oxidizing prokaryotes in soils. *Nature* **17**: 806–809.

Minchin PR (1987) An evaluation of the relative robustness of techniques for ecological ordination. *Plant Ecol* **69**: 89–107.

Moeseneder MM, Arrieta JM, Muyzer G, Winter C & Herndl G (1999) Optimization of terminal-restriction fragment length polymorphism analysis for complex marine bacterioplankton communities and comparison with denaturing gradient gel electrophoresis. *Appl Environ Microb* **65**: 3518–3525.

Nicol GW, Leininger S, Schleper C & Prosser JI (2008) The influence of soil pH on the diversity, abundance and transcriptional activity of ammonia-oxidizing archaea and bacteria. *Environ Microbiol* **10**: 2966–2978.

Öquist MG, Nilsson M, Sörensson F, Kasimir-Klemedtsson A, Persson T, Weslien P & Klemedtsson L (2004) Nitrous oxide production in a forest soil at low temperatures – processes and environmental controls. *FEMS Microbiol Ecol* **49**: 371–378.

Öquist MG, Petrone K, Nilsson M & Klemedtsson L (2007) Nitrification controls N_2O production rates in a frozen boreal forest soil. *Soil Biol Biochem* **39**: 1809–1811.

Pedersen H, Dunkin KA & Firestone M (1999) The relative importance of autotrophic and heterotrophic nitrification in a conifer forest soil as measured by ^{15}N tracer and pool dilution techniques. *Biogeochemistry* **44**: 135–150.

Philippot L (2002) Denitrifying genes in bacterial and archaeal genomes. *Biochim Biophys Acta* **1577**: 355–376.

Prosser JI & Nicol GW (2008) Relative contributions of archaea and bacteria to aerobic ammonia oxidation in the environment. *Environ Microbiol* **10**: 2931–2941.

Rotthauwe JH, Witzel KP & Liesack W (1997) The ammonia monoxygenase structural gene *amoA* as a functional marker: molecular fine-scale analysis of natural ammonia-oxidizing populations. *Appl Environ Microb* **62**: 4704–4712.

Santoro AE, Francis CA, de Sieyes NR & Boehm AB (2008) Shifts in the relative abundance of ammonia-oxidizing bacteria and archaea across physicochemical gradients in a subterranean estuary. *Environ Microbiol* **10**: 1068–1079.

Schär C, Vidale PL, Lüthi D, Frei C, Häberli C, Liniger MA & Appenzeller C (2004) The role of increasing temperature variability in European summer heatwaves. *Nature* **427**: 332–336.

Schimel JP, Firestone M & Killham KS (1984) Identification of heterotrophic nitrification in a Sierran forest soil. *Appl Environ Microb* **48**: 802–806.

Schindlbacher A, Zechmeister-Boltenstern S & Butterbach-Bahl K (2004) Effects of soil moisture and temperature on NO, NO_2, and N_2O emissions from European forest soils. *J Geophys Res* **109**: 1–12.

Schinner F, Öhlinger R, Kandeler E & Margesin R (1996) *Methods in Soil Biology*. Springer Verlag, Berlin.

Shen J, Zhang L, Zhu Y, Zhang J & He J (2008) Abundance and composition of ammonia-oxidizing bacteria and ammonia-oxidizing archaea communities of an alkaline sandy loam. *Environ Microbiol* **10**: 1601–1611.

Stres B, Danevcic T, Pal L *et al.* (2008) Influence of temperature and soil water content on bacterial, archaeal and denitrifying microbial communities in drained fen grassland soil microcosms. *FEMS Microbiol Ecol* **66**: 110–122.

Throbäck IN, Enwall K, Jarvis A & Hallin S (2004) Reassessing PCR primers targeting *nirS*, *nirK* and *nosZ* genes for community surveys of denitrifying bacteria with DGGE. *FEMS Microbiol Ecol* **49**: 401–417.

Tourna M, Freitag TE, Nicol GW & Prosser JI (2008) Growth, activity and temperature responses of ammonia-oxidizing archaea and bacteria in soil microcosms. *Environ Microbiol* **10**: 1357–1364.

Treusch AH, Leininger S, Kletzin A, Schuster SC, Klenk HP & Schleper C (2005) Novel genes for nitrite reductase and Amo-related proteins indicate a role of uncultivated mesophilic Crenarchaeota in nitrogen cycling. *Environ Microbiol* **7**: 1985–1995.

Wallenstein MD, Myrold DD, Firestone M & Voytek M (2006) Environmental controls on denitrifying communities and denitrification rates: insights from molecular methods. *Ecol Appl* **16**: 2143–2152.

Zumft WG (1997) Cell biology and molecular basis of denitrification. *Microbiol Mol Biol R* **61**: 533–616.